

Integral Test of Neutron Data and Comparison of Codes by Re-analysis of the SEG and STEK Experiments

K. Dietze ¹⁾, M. Ishikawa ¹⁾, G. Rimpault ²⁾

¹⁾ JNC - Japan Nuclear Cycle Development Institute, O-arai, Ibaraki-ken, 311-1393, JAPAN

²⁾ CEA – Centre de Etudes Cadarache, DER/SPRC, F – 13108 St.-Paul-lez-Durance, FRANCE

Abstract

Sample reactivity measurements performed at the fast-thermal coupled facilities RRR/SEG (RC Rossendorf) and STEK (ECN Petten) have been re-analyzed using the JNC standard route for reactor calculation JENDL-3.2 // SLAROM / CITATION / PERKY. The C/E-values are compared with results obtained with the competitive European scheme JEF-2.2 // ECCO / ERANOS.

When using different input libraries, codes, self-shielding treatments, and likewise different energy group structures in the routes, it is very difficult to locate exactly the source of deviations in the C/E-values. Therefore, a cross-wise use of JEF-2.2 with JNC codes was performed to obtain separate information about data and codes. Furthermore, test calculations have been made to investigate special effects.

More comparisons of data libraries and routes, desirable in crisscross way, are recommended to overcome specific disadvantages in integral tests.

1. Introduction

Integral tests are necessary to check neutron data and codes used in reactor calculations. Such feedback is very important to evaluators for data corrections, but also to programmers for improvements of the codes.

The NEA NSC Working Group on International Evaluation Cooperation in the OECD countries proposed to use the STEK and SEG experiments, as a joint data base, for the validation and convergence of the last versions of JEF, JENDL, and ENDF/B, especially for capture and inelastic data of fission product nuclides and structural materials [1].

At Cadarache / CEA France, extensive re-analyses of the SEG and STEK experiments have been recently completed using the European analytical scheme for reactor calculation (JEF-2.2 / ECCO / ERANOS). The results are given and discussed in many CEA reports, JEF documents, and publications [2,3,4]. Corrections in JEF data have been recommended based on perturbation theory calculations accompanied and confirmed by adjustment studies [5]. The SEG information has been documented and preserved in the SNEDAX data base.

Similar analyses have been performed now using JFS group data based on JENDL-3.2 as input for the JNC standard route (JENDL-3.2 / SLAROM / CITATION / PERKY) to check the last version of JENDL-3.2. The STEK experiments have been already analyzed with other codes in Japan [6,7], but not the SEG experiments up to now. Unfortunately, the results obtained with the JNC route and European scheme can't be compared directly. When using different input libraries, codes in the routes, self-shielding treatments, and likewise different energy group structures, it is very difficult to locate exactly the source of differences in the results. Therefore, a crisscross use of input libraries and codes is recommended. An attempt was made for the SEG experiments as soon as JFS group data of JEF-2.2 have been available for all materials used in RRR/SEG facilities and for samples.

The present integral tests consist in the interpretation of the C/E-values; i.e., the ratio of the calculated central reactivity worth (CRW) to the experimental, infinitely dilute value. The experimental value was determined extrapolating the measured specific reactivities of the samples to "zero mass" by self-shielding corrections taking into account the real sample sizes. In cases of discrepant C/E-values, calculated maps of reactivity contributions for the reaction types in energy groups are very helpful to find the main contributions and sources of the discrepancy.

2. The fast-thermal coupled facilities SEG and STEK

Both facilities RRR/SEG (Rossendorf/Germany) and STEK (Petten/Netherlands) were zero power reactors and similar in construction. The annular thermal drivers were filled by fuel sections and moderated by water surrounded by a reflector. The inner insertion lattices were loaded with fuel and moderator pellets producing the fast neutron flux. The characteristics of the neutron and adjoint spectra were obtained by special arrangements of these pellets in unit cells. In this way, a hard or soft neutron spectrum or a special energy behavior of the adjoint function could be reached. Between the thermal drivers and the fast insertion lattices, a converter (or buffer) was installed. The samples were oscillated by means of tubes to the central position of the facilities. The constructions of STEK and RRR/SEG are well suited for reactor calculations in R,Z-geometry. The STEK facility is described in detail in [8]. The Rossendorf reactor RRR with the fast insertion lattice SEG [9] and all measurements are well documented [10] and likewise preserved in the SNEDAX data base.

The main differences between the STEK and RRR/SEG facilities consist in the construction materials and in the geometry of pellets. In STEK, stainless steel was used for tanks and oscillation element and square pellets, in SEG pure aluminum for the cylindrical SEG and oscillation tube and circular pellets.

But, there are a lot of peculiarities and differences at both facilities to be considered in the calculations. The neutron and adjoint spectra needed for perturbation calculation were calculated for the critical reactor taking into account the following facts:

1. Thermal driver and converter: The annular thermal driver of the RRR consists of 24 rectangular cassettes filled with fuel sections beginning from inside and graphite in the outer region. Due to the fact that the loading of the cassettes was not uniform (mostly 8 fuel sections, but also 9 or 12) and because graphite wedges were placed between the cassettes, the thermal driver can be divided into two zones with an "effective" borderline. Neutron and adjoint fluxes have been calculated for the "critical thickness" of the thermal driver zone. Usually, a graphite converter was installed. Only in case of SEG-6, natural uranium was used. In STEK, between the inner fast zone and the thermal driver, lead elements, a graphite buffer, and curved control plates of Al-B₄C (8 pieces) were placed. The control plates could be moved up and down. Neutron and adjoint fluxes were calculated for a "critical thickness" of the control plates. Air gaps were smeared.
2. Fast zones: The insertion lattice of the SEG is a cylinder made of aluminum with 72 cylindrical holes. The holes were filled with cylindrical pellets in defined order (unit cells or concentric rings). According to the SEG configuration, pellets of enriched uranium (36% enriched in U-235), natural uranium, graphite, boron-graphite, polyethylene, aluminum, and cadmium were used [9]. In case of STEK, two different regions (inner and outer fast cores) have been arranged. The five STEK cores differ in the ratios of graphite to uranium. STEK-500 with the hardest neutron spectrum contained additional boron as a poison in the outer regions of the fast core. Safety criteria did not allow a uniform C/U-ratio over the whole core. The characteristics of the uranium, graphite, and hiduminium (an aluminum-boron carbon alloy) platelets and the filling scheme of the inner and outer core regions and oscillator elements are given in [8].

3. Sample oscillation: The oscillation element of STEK had a complicated U profile loaded by 53 cubic compartments. All were made of stainless steel and were oscillated in the central (square) fuel element as guiding tube. 51 compartments were loaded with platelets as in the inner core region. Two of the compartments were used for the sample and reference sample located in a distance of the oscillation stroke. The problem for cell calculations is that the near vicinity of the sample was not always clearly defined: capsules, boxes, and air. In case of SEG, the whole aluminum tube was filled with graphite bars. The samples were completely embedded in graphite sample holders and were oscillated against void. Graphite sample holder and the related dummy could be removed and placed through windows in the tube, remote controlled. In this way, there were clear material conditions; i.e., the sample was completely surrounded only by graphite.

The SEG experiments are considered “clean” integral experiments, simple and clear in geometry and well suited for calculation. In all SEG configurations only a few materials were used: Al, C, B-10, B-11, U-235, U-238, and in special cases Cd (SEG-4) and H (SEG-7A). The most of these materials are standards. Due to the designed adjoint function, the capture or scattering effect was dominant, convenient to check separately capture or scattering data. The 5 STEK configurations, on the other hand, cover a broad energy range due to their increasing softness. The experiments are very valuable because of the extensive program of sample reactivity measurements with many FP nuclides important in reactor burn-up calculations.

3. Neutron spectra and adjoint functions

In research reactors used for data testing, the neutron spectra are often chosen to be softer than in typical fast reactors. At the STEK facilities, the neutron spectra (Fig. 1) were softened successively by decreasing the uranium/graphite-ratio. Furthermore, in the hardest configuration STEK-500, even boron was added. The same considerations were made for the SEG facilities: a special boron carbide region was introduced into the center of the SEG-6. And into the unit cells of SEG-7A, thin polyethylene foils were inserted producing a very long soft tail in the neutron spectrum.

The adjoint function of a typical fast reactor is characterized by more or less increasing wings at lower and higher energies. For the SEG experiments, the idea was born to design the adjoint function to check separately capture and scattering data [11]. In case of an energy-independent adjoint spectrum, the slowing-down effect disappears and the sample reactivity is only due to absorption [11,12,13,14]. On the other hand, in configurations with adjoint spectra of strong dependence on energy, the scattering effect is dominant [15]. Such characteristic adjoint spectra are shown in Figures 3 and 4. In order to achieve this behavior, the fact was used that more (less) U-238 increases (decreases) the adjoint function at higher energies and more absorber material decreases it at lower energies. In this way, the adjoint spectra of the SEG were designed by using a precisely defined combination of different pellets in unit cells or concentric rings in the fast insertion lattices.

The SEG-4, SEG-5, and SEG-7A were arranged with unit cells. To decrease the adjoint function in the lower energy region, Cd pellets were added in SEG-4 [11,12], and mixed and pressed B-10/graphite-pellets in SEG-5 [13,14] and SEG-7A [16,17]. The use of B-10 instead of Cd brought an advantage in the accuracy of calculation because the absorption cross-section of B-10 is well known and has no resonances. In SEG-7A, polyethylene pellets were additionally inserted into the unit cell to soften the neutron spectrum.

In case of SEG-6 [15], the Al cylinder was filled with pellets in concentric rings, starting from inside with enriched uranium pellets, natural uranium pellets, and aluminum pellets. Additionally, a uranium converter was placed between Al cylinder and thermal driver. Both SEG-6 versions differ only in the diameter of the experimental channel (EK). EK10 and EK45 were used for samples with diameters up to 10 mm and 45 mm, respectively. The experimental channel (Al tube) was filled with boron carbide surrounded by a stationary absorber zone likewise of boron carbide. The neutron and adjoint spectra in both SEG-6 versions are very similar.

When the adjoint function is monotonously rising as in SEG-6, all scattering contributions are negative. This fact was also used for the SEG-7A. Additionally, the SEG-7A was characterized by a very soft neutron spectrum (see Fig. 5). There are no compensating effects because both capture and scattering contributions are negative. Therefore, the SEG-7A was well suited for measurements with weak absorbers.

Thus, having SEG configurations with hard or soft neutron spectra and with different shapes of the adjoint function, separate information about capture and scattering data could be obtained.

Neutron and adjoint fluxes of all STEK and SEG cores calculated with the JNC standard route for the sample position are shown in Fig. 1 – 5. The fluxes are given according the output of CITATION, without normalization. The corresponding fluxes obtained with the European scheme are given in [2,3,4]. The calculated spectra are not directly comparable because of different energy group structures (JNC route: 70 energy groups, European scheme: 33), but the differences seem to be small.

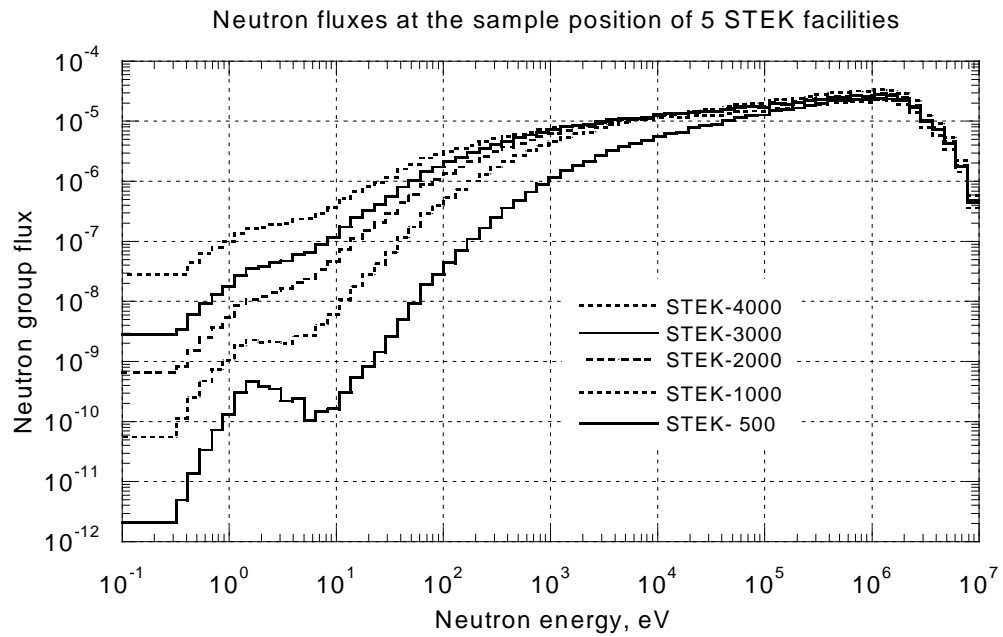


Fig. 1:
Neutron fluxes at the central position of the STEK cores calculated with the JNC standard route

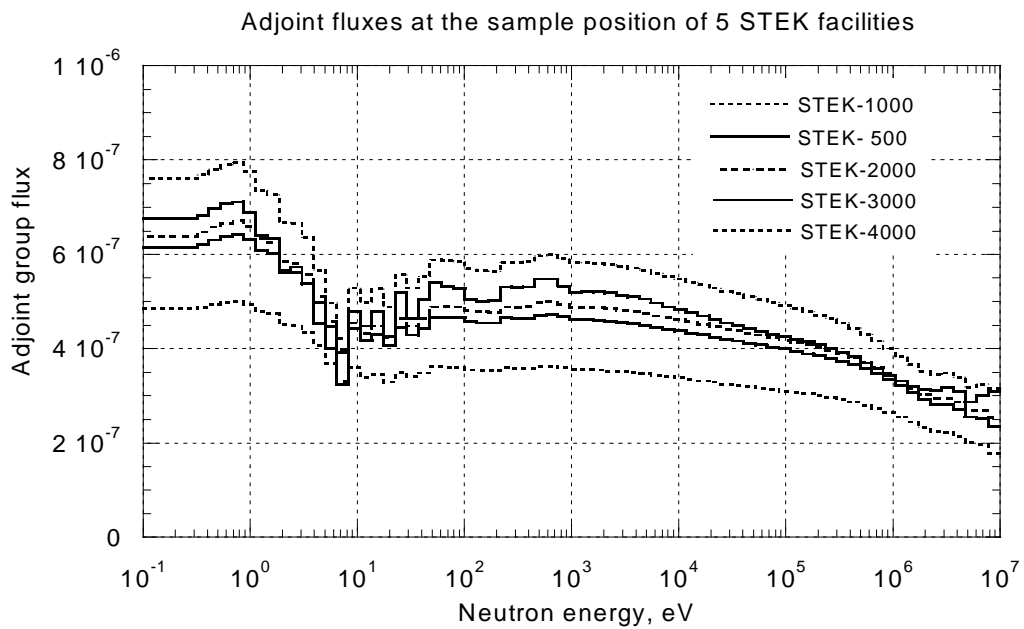


Fig. 2:
Adjoint functions at the central position of the STEK cores calculated with the JNC standard route

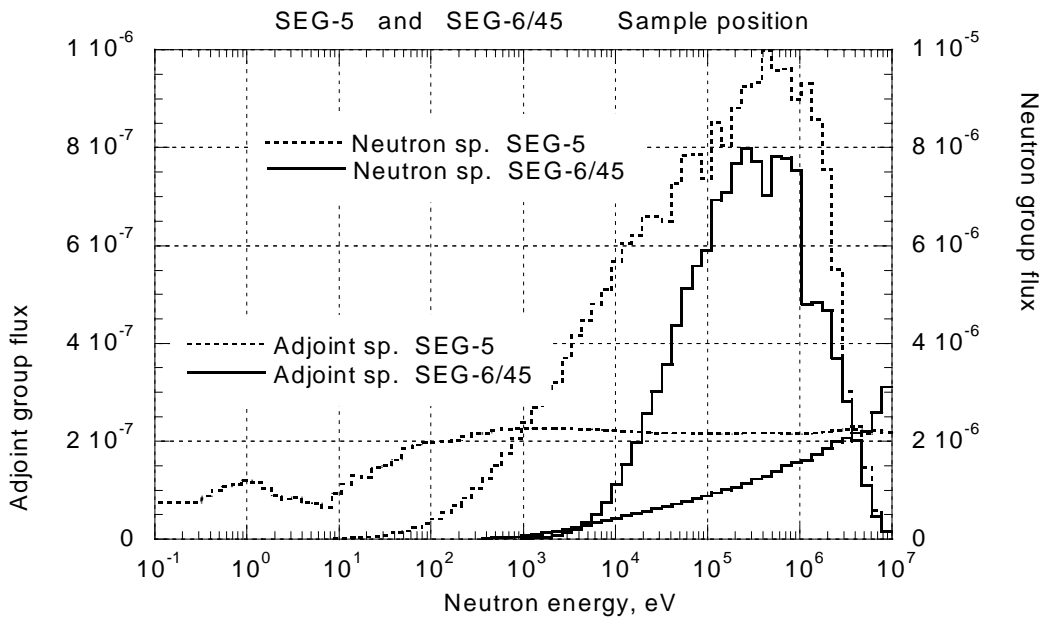


Fig. 3:
Neutron fluxes and adjoint functions at the central position of SEG-5 and SEG-6/45 calculated with the JNC standard route

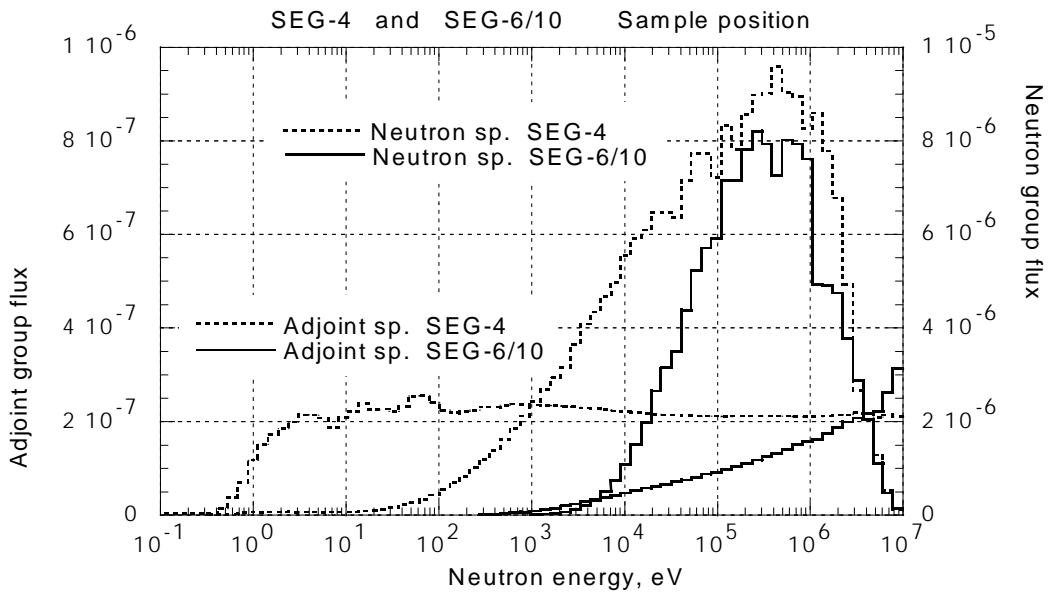


Fig. 4:
Neutron fluxes and adjoint functions at the central position of SEG-4 and SEG-6/10 calculated with the JNC standard route

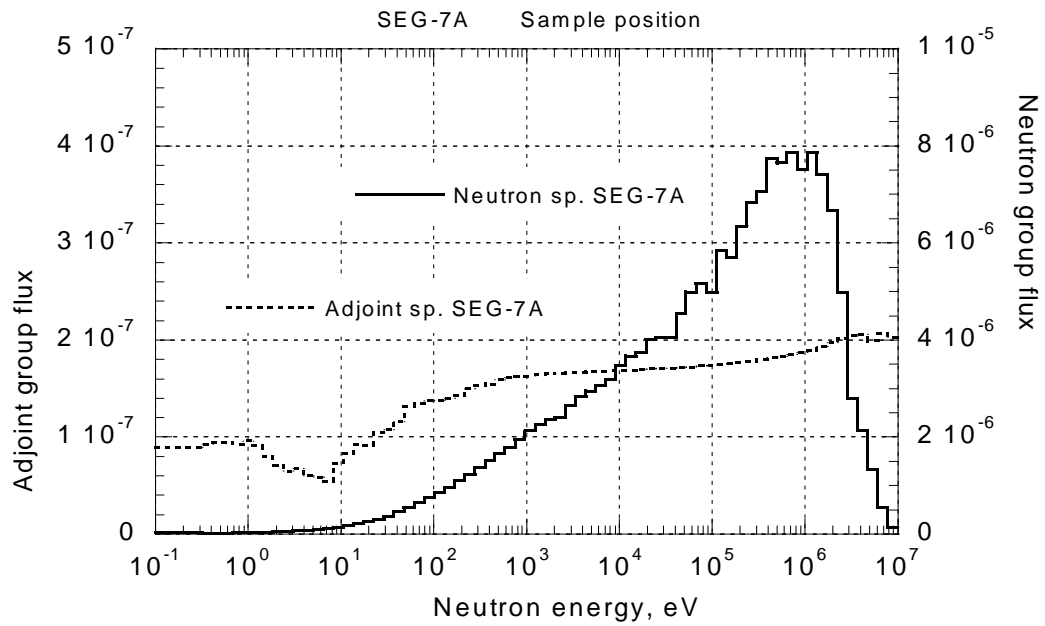


Fig. 5:
 Neutron fluxes and adjoint function at the central position of SEG-7A calculated with the JNC standard route

4. Sample reactivity measurements

In both, SEG and STEK, the sample reactivity measurements were performed using the pile-oscillation method developed to a high perfection [12,14,18]. The most important sample reactivity measurements at SEG are documented in [10] and preserved in the SNEDAX data base. The measured reactivities at STEK are compiled in [18]. Whereas the most oscillation measurements at STEK have been usually performed in 40 minutes and a reactor power of 10 Watt, the measurements at SEG run over 8 hours and more, and with a reactor power of 50 Watt. Consequently, the statistical accuracy of the SEG measurements is much better, especially for small samples. The statistical error of the measurement is the main component in the total error of the C/E-value (see chapter 6).

In integral tests, the calculated and experimental reactivity worths could be compared for real samples or for the infinitely dilute value of the nuclide. Whereas in the first case, the C/E-ratios must be determined for each and every sample, give the second case already a characteristic parameter of the material under investigation. In these analyses, the second case was preferred. But, this characteristic value must be determined by extrapolation to zero mass. This extrapolation is not difficult for materials measured in configurations with hard spectra. In this case, the self-shielding effect is small. In soft spectra, however, small samples have already a considerable self-shielding effect and an experimental extrapolation is not possible. Nevertheless, it was tried to measure the dependence of the specific reactivity on sample size in a wide mass range and down to small effects. Even for exotic fission products, a few samples had been prepared [18,19]. For very small samples, however, the accuracy of the measurements is limited by the reactor noise and by drifts. At SEG, reactivities could be measured down to a few millicents ± 0.3 millicent. Many methodical investigations have been performed concerning accuracy and statistics.

For an appropriate extrapolation to infinitely dilute values (CRW), the dependence of the self-shielding effect on NI (= density x chordlength) has been calculated. In case of SEG, different data libraries and codes were used for this. If code and data are good, the corrected experimental curve should be horizontal. In this way, data and codes used in the calculations of the self-shielding effect could be tested. The procedure of the determination of CRW's in the SEG experiments is described in detail in [12,19]. The same extrapolated values were used in the analyses using the European scheme [2,3]. In case of STEK, new extrapolations were made in a similar way as for SEG. The calculated curves of former analyses [4,20,21,22] have been used for this.

5. Analytical methods

Calculations have been performed using the JNC standard route

- with collapsing procedure (by JOINT) from 70 energy groups to 18 groups,
- without collapsing, all only in 70 groups,
- and with JFS3 data of JEF-2.2 as input for the JNC codes (for SEG only) in 70 groups.

The C/E-values of the SEG experiments were compared to the results obtained with the European scheme [2,3].

5.1 The JNC standard route

In this route, the 70 group library JFS-3 based on JENDL-3.2 [23] and the codes SLAROM, CITATION, JOINT, and PERKY [24,25,26,27] were used. The order of carrying out the calculation is similar to the European scheme JEF-2.2 / ECCO / ERANOS [28,29,30].

At first, cell calculations with SLAROM [24] were performed for all zones using the 70 energy group data as input. Outer zones were treated homogeneously (e.g., the reflectors, converters, and construction elements), but all zones loaded with pellets (insertion lattice of SEG, the core regions and the oscillation element of STEK) were calculated heterogeneously in slab geometry according to the unit cells of the configurations. Unfortunately, the “macro cell method” [2,3] was not applicable.

The PDS files produced by SLAROM were used then in the following calculation with CITATION [25] to determine the neutron and adjoint fluxes in 70 groups. The R,Z-geometry was taken as in former calculations with ECCO / ERANOS [2,3,4] according to the original reports and documentations [8,9,10]. The sample position at the center of the facility was introduced as a separate small cylindrical zone in order to use the route later in calculations for real samples. The neutron and adjoint group fluxes were calculated for the critical condition by small changes of the effective thickness of the thermal driver (SEG) or of the boral control plates (STEK) as described already in chapter 2. The calculated group fluxes are shown in Fig. 1 – 5.

In the next step, first order theory perturbation calculations were performed with PERKY [27], providing total and partial reactivity contributions for all reaction types and energy groups (mapping version).

Finally, the ratios of the calculated to experimental specific reactivity (infinitely dilute worth CRW) were determined by hand for each material under investigation. In order to avoid the determination of the normalization integral of the reactor, the C/E-values were normalized to a reference material, preferably a standard. In most cases boron-10 was used for this. In SEG-6, the scattering effect is dominant; therefore, hydrogen (graphite in the European scheme) was preferred as the reference material.

For the present analysis, the JNC standard route was a little bit modified: elastic and inelastic scattering contributions were separately calculated and given in two columns in the PERKY output.

At first, the calculations were carried out condensing the macroscopic cross-sections and fluxes from 70 energy groups to 18 with JOINT [26]. But, differences were found between the results in 70 and 18 groups [31]. The results in 70 groups show a better agreement (see Tables 2 and 3). Therefore, all final calculations have been made in 70 energy groups then. The collapsing from 70 to 18 or 7 energy groups is not recommended for facilities with soft neutron spectra because of the very broad 18th or 7th energy group (from 10⁻⁵ up to 100.3 eV).

5.2 The European scheme

The calculations with JEF-2.2 / ECCO / ERANOS have been performed in a similar way. The calculational scheme is described in detail in [2,3].

Using the 1968 or 172 group libraries of JEF-2.2 [28], cell calculations with ECCO [29] were performed for each region condensed then to 33 groups for the ERANOS input. The unit cells of with pellet-loaded channels were treated heterogeneously in slab geometry. ERANOS [30] reads the ECCO output files and changes them into EDL's. The R,Z-geometry was used as given in the original reports [8,9,10]. The calculation of the whole reactor was performed then using the diffusion and/or transport code BISTRO (S4 P1 treatment).

The reactivity perturbations of the sample materials at the sample position were calculated by specific moduls of ERANOS. For this, the sample materials were introduced into the experimental channel as traces with an atomic density of 10⁻¹⁰. The calculated reactivities allow to determine C/E-values normalized to a reference material using the extrapolated experimental CRW's.

The European scheme treats the following problems with very good accuracy:

- accurate slowing-down and wide resonance treatment in 1968 energy groups,
- spatial self-shielding treatment with the probability table (subgroup) method,
- macrocell calculation including the surrounding of the sample to treat precisely heterogeneity and resonance interaction effects,
- anisotropic calculation using P1 matrices,
- upscattering calculation for the thermal driver zone.

6. Reference materials and error

In order to avoid the determination of the normalization integral of the reactor, the C/E-values of the materials under investigation were related to a reference material, preferably a standard.

In most cases, boron-10 was used for this because of the high sensitivity to neutron capture in the most SEG and STEK configurations. The experimental values for boron-10 were deducted from measurements with natural and highly enriched boron carbide, and with carbide.

In SEG-6 the scattering effect is dominant; therefore, a scattering material should be used. Preferred candidates are carbon or hydrogen. Hydrogen has been chosen in this analysis, because carbon was present in the immediate vicinity of the sample, as the filling of the experimental channel. The experimental value for hydrogen was deducted from measurements with polyethylene, graphite, and water. Unfortunately, graphite was taken as the reference material for SEG-6 in the European scheme. Consequently, these C/E-values differ for some percents from the results obtained with the JNC route.

The total error of the C/E-values for the SEG experiments was estimated using the following partial errors:

- Statistical error of the measurement with the material,
- Statistical error of the measurement with the reference material,
- The errors of the extrapolation to infinitely dilute values of the sample and reference material,
- The error when the experimental value was deducted from molecular samples,
- The cross-section uncertainty of the reference material,
- An additional error due to uncertainties in compositions and moisture.

The determination of the total error of the C/E-values is described in detail in [19,32].

Of course, the statistical error of the measurements with the sample material is the main source of the total error. Unfortunately, the most measurements at STEK have been performed during 40 minutes only. Consequently, the total error of the C/E-values in STEK experiments (Table 6) is mainly due to the statistical error of the measurement with the sample and was taken from [18]. In many cases, very small effects were measured, sometimes near zero. The calculations show that such small reactivities are often simply the result of a compensating of capture and scattering contributions. Errors of much more than 100 % are unsuitable for interpretation; and negative C/E-values have not been taken into account in the final tables.

7. Special test calculations for the JNC route

Before calculating the final C/E-values, tests have been made for special effects (heterogeneity, favorable energy group structure, calculation of the slowing-down effect, the ratios scattering to capture, etc.) to find the optimal route. The exact treatment of the slowing-down process is very essential, especially for the analysis of measurements with weak absorbers.

Heterogeneity: In the calculations for the final C/E-values, all regions in the vicinity of the sample loaded with pellets have been treated heterogeneously in slab geometry according their unit cells. Additional calculations with the homogenized densities were performed for comparison. Table 1 shows the C/E-values for some sample materials. For the heterogeneous case, the C/E-values (normalized to the C/E-value of boron-10) are mostly within or near the error limit. The homogeneous C/E-values are more discrepant, as expected, especially for the STEK-4000 with the softest spectrum.

Table 1:

Comparison of C/E-values obtained in **homogeneous and heterogeneous** calculations for STEK-1000 and STEK-4000

STEK-1000

MAT	ID	C/E hom	C/E het	Error (%)
B-10	105	1.000	1.000	4
U-235	925	1.075	1.000	5
H	1	1.119	0.996	5
C	6	1.086	0.959	6
Al	13	1.195	1.056	5

STEK-4000

MAT	ID	C/E hom	C/E het	Error (%)
B-10	105	1.000	1.000	4
U-235	925	1.357	1.089	6
H	1	1.139	1.009	7
C	6	1.286	1.033	5
Al	13	1.356	1.046	6

Collapsing procedure: At first, the analyses have been performed using the JNC standard route with the collapsing procedure from 70 energy groups to 18 groups [31]. But, when comparing the results with those of the analysis with the European scheme JEF/ECCO/ERANOS, large differences were found. This could not be explained by data differences alone. Therefore, calculations were made using the JNC route without collapsing; i.e., only in 70 energy groups. In most cases, better results were found especially for sample materials with a considerable scattering contribution and for U-235. In Table 2 and 3, the C/E-values of SEG-5 and SEG-7A are compared for the cases “with and without collapsing”. One of the sources for such differences was found in the very broad 18th energy group covering a large energy range from from 10⁻⁵ until 100.3 eV. Consequently, all further calculations were performed only in 70 energy groups. For all other SEG facilities, similar differences exist between “with and without collapsing procedure” (see tables in [31]).

Table 2:

C/E-values of materials under investigation in **SEG-5**, related to the C/E-value of B-10, obtained with the JNC route, with and without collapsing from 70 to 18 energy groups

Sample Material	ID-No.	CRW exp. (millicent/g)	C/E-value JNC route 70=>18 groups	C/E-value JNC route Only 70 groups	Error (%)
B-10 ss	105	- 1230 ± 20	1.000	1.000	2
Ta	731	- 31.5 ± 1.0	0.921	0.956	7
U-235	925	+ 31.2 ± 2.0	1.321	1.138	10
Mo	42	- 7.4 ± 0.5	1.004	1.031	10
Mn	25	- 12.0 ± 0.5	0.694	0.658	7
Cd	48	- 10.0 ± 0.5	1.060	1.070	9
Nb	413	- 10.0 ± 0.6	1.119	1.072	9
Cu	29	- 4.5 ± 0.5	1.278	1.174	14
Zr	40	- 1.05 ± 0.1	1.397	1.302	13
W	74	- 10.0 ± 0.5	0.877	0.918	8
Fe	26	- 0.7 ± 0.06	1.588	1.342	11
Cr	24	- 0.8 ± 0.06	1.216	1.037	10
Ni	28	- 1.3 ± 0.1	1.561	1.237	10
Co	279	- 20.0 ± 1.5	0.865	1.032	10
B-10 fp	105	- 1174 ± 20	1.000	1.000	2
Mo-95	425	- 14.5 ± 1.0	1.085	1.185	10
Mo-97	427	- 14.0 ± 1.0	1.006	0.980	10
Mo-98	428	- 5.0 ± 0.6	1.115	1.035	15
Mo-100	420	- 4.1 ± 0.5	1.031	0.996	16
Rh-103	453	- 27.0 ± 1.0	0.925	0.899	7
Pd-105	465	- 30.2 ± 1.0	1.136	1.117	7
Ag-109	479	- 31.5 ± 1.5	0.863	0.886	8
Cs-133	553	- 19.5 ± 2.0	0.889	0.909	13
Nd-143	603	- 16.0 ± 1.0	0.835	0.882	9
Nd-145	605	- 18.0 ± 1.0	1.008	1.020	9
Sm-149	629	- 83 ± 5	0.938	1.023	9
Eu-153	633	- 75 ± 5	1.031	1.059	10

Table 3:
C/E-values of materials under investigation in **SEG-7A**, related to the C/E-value of B-10, obtained with the JNC route, with and without collapsing from 70 to 18 energy groups

Sample Material	ID-No.	CRW exp. (millicent/g)	C/E-value JNC route 70=>18 groups	C/E-value JNC route Only 70 groups	Error (%)
B-10	105	- 850 ± 10	1.000	1.000	2
C	6	- 1.9 ± 0.05	1.377	1.035	6
U-235	925	+ 28.0 ± 3.0	1.208	1.149	13
Ta	731	- 26.0 ± 1.0	0.861	0.868	7
Mo-95	425	- 16.8 ± 2.5	0.812	0.940	18
Mo-97	427	- 8.0 ± 0.6	0.993	0.956	11
Mo-98	428	- 2.7 ± 1.0	1.264	1.133	40
Mo-100	420	- 8.1 ± 1.0	0.324	0.300	13
Rh-103	453	- 15.0 ± 2.0	1.199	1.168	16
Ag-109	479	- 36.0 ± 1.5	0.911	0.820	7
Sm-149	629	- 70.0 ± 3.0	1.601	1.751	7

Sample slowing-down effect: The total scattering effect is calculated by addition of all group contributions of elastic and inelastic scattering reactions. For this, the group matrix of the inelastic cross-sections and the elastic removal cross-sections are used, both weighted by the neutron group fluxes and the difference of the adjoint fluxes in the groups between the neutrons are scattered down. The positive or negative sign of the group contribution should follow accordingly if the neutrons are scattered into an energy group of higher or lower importance, respectively.

Because of the complicated behavior of the adjoint function at STEK facilities (Fig. 2), the calculated scattering effect is the sum of all negative and positive contributions. Therefore, it was more convenient to investigate this effect for SEG facilities. Due to the monotonously rising adjoint function of the SEG-6 (see Fig. 3 and 4), the scattering effect is dominant and all contributions are negative. Table 4 shows the absolute contributions due to the different reactions in SEG-6/45. The leakage term is very small at the sample position and is not given in the table. The C/E-values of sample materials with small scattering contribution (B-10, U-235) might be distorted. Graphite also should be treated carefully because it was present in the near vicinity of the sample. Due to the hard neutron spectrum, the SEG-6 is very suitable for tests of inelastic scattering data.

Table 4:
Contributions of different reactions to the total reactivity of samples in SEG-6/45 using the JNC standard route

Sample Material	C/E-value JNC route 70g	Error (%)	Capture (%)	El. Scatt. (%)	Inel. Scatt. (%)	Fission (%)
H	1.000	5	0.004	100.0	0.0	0.0
C	0.918	8	0.46	98.4	1.2	0.0
B-10	0.823	12	89.6	9.8	0.6	0.0
Mo	0.935	7	25.6	11.5	62.7	0.0
Fe	0.925	7	9.0	25.5	65.5	0.0
Cr	0.887	7	6.5	35.5	58.1	0.0
Ni	0.986	9	32.7	37.7	30.1	0.0
Al	1.109	8	3.5	68.6	28.0	0.0
Zr	0.918	8	10.0	23.9	66.0	0.0
Ti	0.911	8	6.5	45.3	48.2	0.0
Cd	0.802	7	39.5	6.9	53.3	0.0
Pb	1.166	12	2.7	11.8	84.2	0.0
Bi	0.911	12	4.2	14.7	79.7	0.0
Mg	1.082	13	3.4	73.3	23.4	0.0
Be	1.186	7	6.4	79.9	13.7	0.0
W	0.926	9	24.8	3.6	70.7	0.0
Cu	1.046	8	18.6	21.7	59.8	0.0
Mn	0.896	8	6.8	32.2	61.0	0.0
Ta	0.874	7	50.0	2.3	47.4	0.0
V	0.934	9	5.0	45.7	49.4	0.0
Si	0.893	11	6.1	68.4	25.7	0.0
Nb	0.943	8	28.3	12.1	59.6	0.0
Co	1.119	8	9.5	28.9	61.7	0.0
U-235	0.898	7	6.8	0.3	6.0	113.2
U-238	0.906	12	57.7	5.4	115.7	81.0
Th-232	0.858	9	38.6	3.1	65.5	8.7

Scattering to total reactivity ratio: For this problem, the SEG-5 experiments have been preferred. Due to the nearly energy-independent adjoint function (Fig. 3), the capture reactivity is dominant and the scattering effect should be very small. In Table 5, the ratios “scattering to total” are compiled for different routes. A positive sign means that both, capture and scattering term are negative. The scattering effect calculated with the European scheme (last column) is mostly less than 1%, either positive or negative. This is expected because of the slight depression in the adjoint function. Only for Fe, Cr, and Ni, a larger positive scattering effect was calculated. In contrast, the JNC route in 70 groups (column before) only gives nearly negative slowing-down effects (except for Ni) and most are very much larger. Considerable contributions are coming from the upper energy groups. Furthermore, the scattering effects obtained with collapsing from 70 to 18 groups are much more larger (first and second column), even if JEF-2.2 is used as input data. As a consequence of all this, the calculation procedure for the slowing-down effect in PERKY or the generated JFS3 data used in the calculation should be checked. Unfortunately, the adjoint functions calculated with different routes could not compared directly to exclude this source.

Table 5:
Ratios of the scattering to the total reactivity obtained with different routes for SEG-5

Sample Material	Scat./ Tot. (%) JNC route 70=>18g JENDL/JNC codes	Scat./ Tot. (%) Cross-wise 70=>18g JEF/JNC codes	Scat./ Tot. (%) JNC route 70g JENDL/JNC codes	Scat./ Tot. (%) Europ. scheme 1968,172,33=>33g JEF/ECCO/ERANOS
B-10	+0.10	+0.08	+0.01	-0.012
Ta	+0.45		+0.26	-0.02
U-235	-0.17	-0.19	-0.12	+0.008
Mo	+2.5	+2.9	+1.5	+0.12
Mn	+9.3	+4.5	+3.9	+0.12
Cd	+1.2		+0.76	-0.14
Nb	+1.6		+0.97	-0.05
Cu	+5.4	+4.8	+1.5	-0.61
Zr	+7.5	+9.1	+4.8	-0.27
W	+3.8		+1.2	+0.10
Fe	+19.6	+20.8	+9.7	-8.0
Cr	+12.8	+14.4	+2.7	-12.3
Ni	+11.2	+11.9	-4.5	-11.1
Co	+1.5		+2.9	+0.21
Mo-95	+1.1		+0.75	+0.64
Mo-97	+1.3		+0.77	-0.12
Mo-98	+6.3		+2.5	+0.01
Mo-100	+3.4		+2.9	-0.12
Rh-103	+0.6		+0.38	-0.07
Pd-105	+0.4		+0.28	-0.07
Ag-109	+0.5		+0.31	-0.03
Cs-133	+0.6		+0.43	-0.03
Nd-143	+1.0		+0.55	+0.99
Nd-145	+2.0		+0.44	+0.81
Sm-149	+0.2		+0.09	+0.02
Eu-153	+0.2		+0.10	-0.01

8. C/E-values and discussion

Before starting the calculations for all materials under investigation, tests were performed to assure that the C/E-values of standards and a few other materials with well-known cross-sections differ only within the limits of their data accuracies and experimental errors (i.e., not more than about 5 ... 6%) when related to the C/E-value of the normalization material. This was a prerequisite for the analysis of all other materials, especially of weak absorbers with small reactivity effects.

The C/E-values of the central reactivity worths (CRW) for all STEK and SEG facilities are compiled in the Tables 6 - 11. The determination of the experimental (extrapolated infinitely dilute) CRW's was described in the last paragraph of chapter 4. The C/E-values of the STEK configurations are sensitive according to the softness of their neutron spectrum, whereas the C/E-values of the SEG configurations give separate information about capture or scattering data. The SEG-4 and SEG-5 are highly sensitive to capture and both SEG-6 versions to inelastic or elastic scattering data according Table 5. Because of the very soft neutron spectrum in the SEG-7A, the results of materials with large thermal and epithermal cross-sections should be treated carefully (e.g., Sm-149). The same was found in the results obtained with the European route. Furthermore, the results for materials present in the vicinity of the sample (Graphite and Aluminum in the SEG, and stainless steel components and Aluminum in STEK) could probably be doubtful in how far the resonance interaction is exactly taken into account in the calculation. In ECCO, this interaction is treated by macrocell calculations.

For most standards and strong absorbers, a good agreement in the C/E-values exists. But many discrepancies were found for a lot of weak absorbers and structural materials with considerable scattering proportion (e.g., for the main stainless steel components Fe, Cr, Ni). Obvious discrepancies have been highlighted in the Tables 6 - 11. The data of these materials should be checked or reviewed. Often there are simple errors in the generated JFS3 group data.

Table 6 shows the C/E-values and their errors for all STEK facilities obtained with the JNC route in 70 energy groups. Significant discrepancies were found for nearly all isotopes of Zr and for Mo-98, Mo-100, Tc-99, Ag-109, Cs-133, and Sm-151 as important FP nuclides in fast reactor calculations. The 22 most important FP nuclides for fast reactor calculation, contributing about 85% to the total reactivity effect of all FP nuclides, are marked as 'Important FP'. They are mostly strong absorbers. Pb is overestimated in all STEK configurations and likewise in both SEG-6 versions. The scattering data should be checked. The C/E-values for Pu-240 are overestimated. This fact is confirmed by calculated averaged transmissions [33]. JENDL-3.2 of Pu-240 has larger total cross-sections in the fast energy region compared with other evaluations. The C/E-values for STEK can be compared with results using the European scheme, presented in a separate JEF/DOC [4]. In this report, three independent methods have been used to tackle the important self-shielding problem of the sample. A. Meister's third approach is comparable with the extrapolation method used in this work.

Table 7 and 8 show the C/E-values for SEG-4 and SEG-5. The sample reactivity is nearly due to capture. There are compared the values of the JNC route with those of the European scheme, and with results of the cross-wise use of JEF-2.2 as input for JNC codes. The following conclusions can be given for capture data:

- Mn is clearly underestimated in JENDL-3.2. Because the reactivity is mainly due to the energy groups with the main resonances, these data should be checked.
 - JENDL-3.2: Ag-109 and W seem to be underestimated,
 - JEF-2.2: Cd and Sm-149 are overestimated, Mo-100 and Ag-109 underestimated.
- The overestimation of Fe, Cr, Ni, and Zr of JENDL-3.2 is not understandable; it could probably be interpreted as result of the scattering contributions, because this is not so far seen for the European scheme. Larger effects with a trend to negative signs were calculated for the scattering effect (Table 5).

Both SEG-6 facilities were very sensitive to scattering data. The C/E-values are given in Tables 9 and 10. Discrepancies are found as follows:

- Cd is underestimated, Pb overestimated in JENDL-3.2,
- Be is overestimated in both, JENDL-3.2 and JEF-2.2,
- Zr and Fe are underestimated in both, JENDL-3.2 and JEF-2.2,
- Cd, Si, and Co is overestimated in JEF-2.2.

Noteworthy, that there is a difference of some percent when comparing with the results of the European scheme due to the normalization to H or C in both routes.

In Table 11 (SEG-7A), discrepant results have been found for

- Ag-109 and Mo-100; i.e., an underestimation for both libraries. Capture and inelastic data should be checked.
- The C/E-value of Cd for JEF-2.2 is overestimated as found likewise in SEG-5.
- The overestimation of Sm-149 could be due to the large thermal cross-section and the long tail in the neutron spectrum with contributions down to the thermal region (Fig. 5).

The so-called “U-235 / B-10 discrepancy” in sample reactivity measurements is confirmed only for SEG-5 and SEG-7A, not for STEK. This discrepancy was found in former analyses (e.g., SNEAK, ZEBRA, BFS, ZPR, KBR, etc.); i.e., the C/E-values of U-235, normalized to the C/E-value of B-10 are overestimated, mostly outside of experimental errors and the data uncertainty [34, p.123]. This effect is independent of fuel loading or neutron spectrum softness [10, p.51] and not understandable. As a consequence, the normalization was made to a standard of similar behavior in this work (see chapter 6). Therefore, this overestimation was not found in SEG-6/45, because the C/E-values were normalized to hydrogen.

Table 6:

C/E-values of infinitely dilute sample reactivities in STEK, normalized to the C/E-value of boron-10, obtained with the JNC standard route in 70 energy groups

MAT	ID	STEK-4000	STEK-3000	STEK-2000	STEK-1000	STEK-500	Comment
B-10	105	1.00 ± 4%	1.00 ± 5%	1.00 ± 4%	1.00 ± 4%	1.00 ± 4%	Normalization
H	1	1.01 ± 7%	0.96 ± 6%	0.97 ± 6%	1.00 ± 5%	0.98 ± 6%	Standard
C	6	1.03 ± 5%	0.93 ± 6%	0.94 ± 8%	0.96 ± 6%	0.94 ± 6%	Standard
O	8	0.91 ± 20%	0.96 ± 7%	0.93 ± 6%	0.96 ± 5%	1.01 ± 6%	
Al	13	1.05 ± 6%	0.97 ± 8%	0.99 ± 8%	1.06 ± 5%	1.07 ± 7%	
Si	14	0.87 ± 6%	0.77 ± 13%	0.78 ± 12%	0.84 ± 6%	-	!
Cl	17	1.09 ± 9%	1.13 ± 9%	1.32 ± 12%	1.53 ± 13%	1.11 ± 14%	
V	23	x	0.54 ± 8%	0.59 ± 8%	0.73 ± 8%	-	Small effect, !
Cr	24	x	0.41 ± 7%	0.47 ± 9%	0.56 ± 8%	-	Small effect, !
Fe	26	x	0.38 ± 10%	0.50 ± 8%	0.70 ± 7%	0.86 ± 6%	Small effect, !
Zr-90	400	0.58 ± 29%	0.78 ± 28%	0.71 ± 28%	0.75 ± 24%	0.89 ± 21%	Small effect, !
Zr-91	401	1.51 ± 13%	1.37 ± 15%	1.43 ± 15%	1.22 ± 22%	1.24 ± 68%	!
Zr-92	409	x	x	0.31 ± 55%	0.60 ± 31%	0.72 ± 25%	Small effect, !
Zr-93	403	0.32 ± 43%	0.40 ± 59%	0.37 ± 54%	0.28 ± 57%	0.35 ± 44%	!
Zr-96	406	2.20 ± 28%	x	2.36 ± 79%	1.13 ± 63%	0.86 ± 29%	Small effect
Nb	413	1.05 ± 8%	1.06 ± 10%	1.08 ± 9%	1.06 ± 7%	1.01 ± 6%	Absorber
Mo	42	1.02 ± 8%	0.98 ± 9%	1.04 ± 12%	0.99 ± 10%	0.98 ± 11%	Absorber
Mo-92	422	1.08 ± 48%	1.01 ± 61%	0.97 ± 54%	0.66 ± 53%	x	
Mo-94	424	x	0.66 ± 49%	0.85 ± 37%	1.62 ± 70%	0.37 ± 60%	Small effect
Mo-95	425	0.80 ± 12%	0.81 ± 14%	0.87 ± 14%	0.88 ± 13%	0.82 ± 16%	Important FP, ?
Mo-96	426	1.04 ± 36%	0.91 ± 57%	0.96 ± 50%	1.17 ± 51%	x	Small effect
Mo-97	427	0.77 ± 16%	0.79 ± 15%	0.93 ± 12%	0.97 ± 9%	0.99 ± 13%	Important FP
Mo-98	428	2.33 ± 12%	1.69 ± 20%	2.14 ± 23%	x	x	Important FP, !
Mo-100	420	1.87 ± 15%	1.75 ± 27%	x	x	x	Important FP, !
Tc-99	439	0.84 ± 11%	0.66 ± 12%	0.69 ± 15%	0.72 ± 17%	0.88 ± 8%	Important FP, !
Ru-101	441	1.16 ± 12%	0.99 ± 13%	1.03 ± 13%	0.98 ± 14%	1.04 ± 11%	Important FP
Ru-102	442	0.67 ± 27%	1.05 ± 20%	1.10 ± 19%	1.43 ± 23%	1.95 ± 61%	Important FP, ?
Ru-104	444	1.09 ± 38%	1.09 ± 32%	1.23 ± 39%	1.84 ± 36%	1.24 ± 38%	Important FP
Rh-103	453	0.95 ± 8%	0.97 ± 9%	0.93 ± 9%	0.92 ± 7%	0.90 ± 11%	Important FP
Pd-104	464	1.30 ± 45%	1.46 ± 44%	1.55 ± 47%	1.40 ± 52%	1.58 ± 84%	?
Pd-105	465	0.88 ± 10%	0.85 ± 12%	0.96 ± 10%	1.03 ± 9%	0.99 ± 9%	Important FP
Pd-106	466	1.59 ± 16%	1.47 ± 17%	1.44 ± 15%	1.40 ± 19%	1.43 ± 29%	!
Pd-107	467	0.93 ± 9%	0.92 ± 10%	1.07 ± 11%	1.11 ± 11%	1.04 ± 9%	Important FP
Pd-108	468	0.97 ± 23%	0.81 ± 17%	0.95 ± 22%	1.39 ± 42%	1.17 ± 39%	Important FP
Pd-110	460	1.05 ± 36%	x	0.89 ± 86%	0.59 ± 40%	x	
Ag-109	479	0.78 ± 11%	0.55 ± 13%	0.84 ± 15%	0.72 ± 19%	0.76 ± 14%	Important FP, !
Cd-111	481	0.95 ± 24%	1.10 ± 25%	1.07 ± 22%	0.89 ± 21%	0.95 ± 22%	
Te-128	528	x	x	x	x	0.54 ± 28%	Small effect, !
Te-130	533	x	x	0.79 ± 44%	1.02 ± 39%	x	Small effect
I-127	537	0.73 ± 11%	0.82 ± 17%	0.92 ± 14%	0.87 ± 16%	0.81 ± 20%	?
I-129	539	0.86 ± 28%	0.88 ± 29%	0.93 ± 28%	1.08 ± 21%	1.12 ± 26%	Important FP
Cs-133	553	0.65 ± 10%	0.58 ± 13%	0.70 ± 9%	0.80 ± 8%	0.71 ± 12%	Important FP, !
Cs-135	555	x	0.43 ± 70%	0.61 ± 84%	0.71 ± 85%	0.23 ± 84%	Large err., ?
La-139	579	1.17 ± 8%	1.35 ± 55%	x	x	0.81 ± 53%	Small effect
Ce-140	580	1.54 ± 64%	0.55 ± 54%	0.68 ± 39%	0.98 ± 24%	0.49 ± 45%	Small effect
Ce-142	582	x	0.44 ± 65%	0.27 ± 25%	0.36 ± 19%	0.33 ± 17%	!
Pr-141	591	0.99 ± 19%	1.06 ± 25%	0.87 ± 21%	1.49 ± 29%	0.80 ± 38%	Important FP

continued

Nd-142	602	x	0.76 ±69%	0.98 ±47%	0.73 ±40%	0.93 ±54%	Small effect
Nd-143	603	0.66 ±18%	0.84 ±25%	0.86 ±25%	0.99 ±14%	0.88 ±24%	Important FP
Nd-144	604	0.36 ±37%	0.58 ±45%	0.92 ±54%	0.85 ±44%	x	
Nd-145	605	0.47 ±25%	0.58 ±28%	0.71 ±22%	0.87 ±18%	0.90 ±22%	Important FP
Nd-146	606	0.82 ±37%	0.87 ±72%	1.58 ±84%	x	x	Small effect
Nd-148	608	0.76 ±23%	0.79 ±24%	0.92 ±18%	1.13 ±19%	x	
Nd-150	600	0.75 ±33%	0.92 ±49%	1.30 ±25%	1.69 ±23%	x	
Pm-147	617	0.78 ±19%	0.65 ±24%	0.76 ±21%	0.86 ±15%	0.89 ±12%	Important FP
Sm-147	627	0.86 ±15%	0.87 ±24%	1.11 ±24%	0.95 ±12%	0.96 ±14%	
Sm-148	628	0.49 ±25%	0.59 ±52%	0.90 ±33%	1.23 ±36%	1.54 ±84%	
Sm-149	629	1.25 ±14%	0.89 ±15%	0.87 ±14%	0.88 ±13%	1.05 ±10%	Important FP
Sm-150	620	0.86 ±19%	0.75 ±25%	0.77 ±21%	0.81 ±22%	0.89 ±21%	
Sm-151	621	0.46 ±60%	0.42 ±54%	0.44 ±51%	0.50 ±53%	0.55 ±55%	Important FP, !
Sm-152	622	0.80 ±25%	0.69 ±39%	0.75 ±27%	0.78 ±26%	0.92 ±37%	
Sm-154	624	0.77 ±27%	0.85 ±38%	0.99 ±32%	1.00 ±28%	0.84 ±46%	
Eu-151	631	0.84 ±14%	0.72 ±17%	0.80 ±16%	0.86 ±12%	0.81 ±17%	From Eu-nat
Eu-153	633	0.92 ±11%	0.94 ±16%	1.02 ±14%	0.99 ±12%	0.98 ±13%	Important FP
Gd-156	646	1.69 ±18%	1.89 ±28%	1.43 ±25%	0.98 ±27%	1.17 ±63%	?
Gd-157	647	3.19 ± 8%	1.41 ±11%	1.24 ±12%	0.99 ±14%	1.23 ±21%	?
Tb-159	659	0.96 ± 6%	0.92 ±13%	1.01 ± 7%	1.08 ± 8%	1.10 ±12%	
Hf	72	1.27 ±11%	1.00 ±18%	0.99 ±14%	0.98 ±11%	1.02 ±13%	Absorber
W	74	0.69 ±13%	-	0.90 ±15%	0.87 ±12%	0.80 ±24%	Absorber
Pb	82	1.67 ± 7%	1.98 ± 9%	1.53 ±13%	1.55 ± 7%	1.72 ± 6%	Small effect, !
Th-232	902	1.64 ± 7%	-	-	1.32 ±10%	-	!
U-235	925	1.09 ± 6%	0.98 ± 7%	0.96 ± 6%	1.00 ± 5%	1.01 ± 5%	Standard
U-236	926	1.27 ±12%	-	-	0.81 ±29%	-	
U-238	928	0.87 ±15%	0.90 ±20%	1.11 ±22%	1.41 ±24%	x	
Pu-239	949	1.13 ± 8%	0.94 ± 8%	0.96 ± 7%	1.01 ± 8%	1.03 ± 7%	
Pu-240	940	1.62 ±20%	1.65 ±45%	1.28 ±53%	x	-	Large err., ?

The errors were estimated and based mainly on the experimental (statistical) error given in ECN-10 [18]

- no measurement (or CRW) was found in reports.
- x measured reactivity or the infinitely dilute values are very small or near zero
- ! Discrepancy, significant
- ? Discrepancy, questionable

Table 7:

C/E-values of infinitely dilute sample reactivities in SEG-5, normalized to the C/E-value of boron-10, obtained with the JNC standard route, the European scheme, and a cross-wise use of JEF-2.2 with JNC codes

Sample Material	ID-No.	C/E-values 70g JNC route JENDL/JNC codes	C/E-values 70g Cross-wise JEF/JNC codes	C/E-values 33g European scheme JEF/ECCO/ERANOS	Error (%)
B-10 ss	105	1.000	1.000	1.000	2
Ta	731	0.956	0.933	0.956	7
U-235	925	1.138	1.124	1.084	10
Mo	42	1.031	0.984	0.964	10
Mn	25	0.658	0.942	0.952	7
Cd	48	1.070	1.214	1.215	9
Nb	413	1.072	1.048	1.022	9
Cu	29	1.174	1.214	1.119	14
Zr	40	1.302	1.085	1.032	13
W	74	0.918	1.019	1.085	8
Fe	26	1.342	1.232	1.084	11
Cr	24	1.037	1.095	1.032	10
Ni	28	1.237	1.185	1.073	10
Co	279	1.032	1.076	0.992	10
B-10 fp	105	1.000	1.000	1.000	2
Mo-95	425	1.185	1.194	1.133	10
Mo-97	427	0.980	0.994	0.954	10
Mo-98	428	1.035	1.039	1.061	15
Mo-100	420	0.996	0.923	0.888	16
Rh-103	453	0.899	0.914	0.901	7
Pd-105	465	1.117	1.077	1.064	7
Ag-109	479	0.886	0.926	0.929	8
Cs-133	553	0.909	0.912	0.926	13
Nd-143	603	0.882	0.897	0.896	9
Nd-145	605	1.020	1.018	1.066	9
Sm-149	629	1.023	1.121	1.191	9
Eu-153	633	1.059	1.068	1.091	10

Table 8:

C/E-values of infinitely dilute sample reactivities in SEG-4, normalized to the C/E-value of boron-10, obtained with the JNC standard route, the European scheme, and a cross-wise use of JEF-2.2 with JNC codes

Sample Material	ID-No.	C/E-values 70g JNC route JENDL/JNC codes	C/E-values 70g Cross-wise JEF/JNC codes	C/E-values 33g European scheme JEF/ECCO/ERANOS	Error (%)
B-10	105	1.000	1.000	1.000	2
U-235	925	0.950	0.980	0.965	10
U-238	928	1.260	1.242	1.056	10
Ta	731	0.922	0.884	0.851	8
Mo	42	1.208	1.153	0.906	12
Nb	413	1.039	1.049	0.889	10
Mn	25	0.826	1.214	0.957	11
Fe	26	1.340	1.388	1.086	12
Cr	24	1.167	1.291	1.076	10
Ni	28	1.067	1.104	1.091	11
Cd	48	1.296	1.502	1.046	10
Cu	29	1.030	1.093	0.878	11
Zr	40	1.192	1.051	0.911	12
W	74	0.823	0.876	0.896	10
Mo-95	425	1.121	1.151	0.913	10
Mo-97	427	1.106	1.142	0.952	9
Mo-98	428	0.856	0.891	0.773	12
Mo-100	420	0.995	0.966	0.803	13
Rh-103	453	1.096	1.132	1.056	12
Pd-105	465	1.031	1.013	0.882	19
Ag-109	479	0.777	0.846	0.809	12
Cs-133	553	1.000	0.985	1.038	13
Sm-149	629	1.057	1.137	1.094	9
Eu-153	633	1.009	0.992	1.108	10

Table 9:

C/E-values of infinitely dilute sample reactivities in SEG-6/45, normalized to the C/E-value of hydrogen (European scheme: graphite), obtained with the JNC standard route, the European scheme, and a cross-wise use of JEF-2.2 with JNC codes

Sample Material	ID-No.	C/E-values 70g JNC route JENDL/JNC codes	C/E-values 70g Cross-wise JEF/JNC codes	C/E-values 33g European scheme JEF/ECCO/ERANOS	Error (%)
H	1	1.000	1.000	1.071	5
C	6	0.918	0.959	1.000	8
B-10	105	0.823	0.821	0.896	12
Mo	42	0.935	0.898	0.913	7
Fe	26	0.925	0.952	0.916	7
Cr	24	0.887	0.977	0.915	7
Ni	28	0.986	1.096	1.133	9
Al	13	1.109	1.202	1.032	8
Zr	40	0.918	0.859	0.860	8
Ti	22	0.911	0.881	0.921	8
Cd	48	0.802	1.026	1.105	7
Pb	82	1.166	0.883	0.913	12
Bi	839	0.911	0.986	1.016	12
Mg	12	1.082	1.014	1.094	13
Be	4	1.186	1.138	1.323	7
W	74	0.926	0.912	0.942	9
Cu	29	1.046	1.063	1.095	8
Au	79		0.919	0.963	9
Mn	25	0.896	1.045	1.076	8
Ta	731	0.874	0.834	0.895	7
V	23	0.934	1.034	1.016	9
Si	14	0.893	1.049	1.207	11
Nb	413	0.943	0.900	0.955	8
Co	279	1.119	1.184	1.241	8
U-235	925	0.898	0.907	0.978	7
U-238	928	0.906	0.881	0.923	12
Th	902	0.858	0.832	0.865	9

Table 10:

C/E-values of infinitely dilute sample reactivities in SEG-6/10, normalized to the C/E-value of hydrogen (European scheme: graphite), obtained with the JNC standard route, the European scheme, and a cross-wise use of JEF-2.2 with JNC codes

Sample Material	ID-No.	C/E-values 70g JNC route JENDL/JNC codes	C/E-values 70g Cross-wise JEF/JNC codes	C/E-values 33g European scheme JEF/ECCO/ERANOS	Error (%)
H	1	1.000	1.000	1.067	5
C	6	0.913	0.952	1.000	9
B-10	105	0.937	0.937	0.973	10
Mo	42	1.008	0.965	0.965	6
Fe	26	0.905	0.928	0.890	6
Ni	28	0.973	1.081	1.121	8
Al	13	1.012	1.096	0.942	7
Zr	40	0.904	0.842	0.836	7
Ti	22	1.043	1.009	1.062	7
Cd	48	0.869	1.103	1.155	6
Pb	82	1.328	1.008	1.028	11
Bi	839	0.910	0.985	0.998	11
Mg	12	1.027	0.961	1.040	11
Be	4	1.180	1.130	1.312	6
W	74	0.956	0.941	0.949	8
Cu	29	1.049	1.064	1.075	7
Rh	453	1.015	1.007	1.049	9

Table 11:

C/E-values of infinitely dilute sample reactivities in SEG-7A, normalized to the C/E-value of boron-10, obtained with the JNC standard route, the European scheme, and a cross-wise use of JEF-2.2 with JNC codes

Sample Material	ID-No.	C/E-values 70g JNC route JENDL/JNC codes	C/E-values 70g Cross-wise JEF/JNC codes	C/E-values 33g European scheme JEF/ECCO/ERANOS	Error (%)
B-10	105	1.000	1.000	1.000	2
C	6	1.035	1.041	1.091	6
U-235	925	1.149	1.144	1.150	13
Ta	731	0.868	0.867	0.928	7
Cd	48			1.304	15
Mo-95	425	0.940	1.050	0.960	18
Mo-97	427	0.956	0.982	0.961	11
Mo-98	428	1.133	1.164	1.141	40
Mo-100	420	0.300	0.286	0.471	13
Rh-103	453	1.168	1.230	1.118	16
Ag-109	479	0.820	0.901	0.894	7
Sm-149	629	1.751	1.337	1.498	7

9. Conclusions

The JNC standard route was used for integral tests of JENDL-3.2 data using sample reactivity measurements performed at 5 SEG and 5 STEK facilities. These facilities were characterized by either neutron spectra with increasing softness (STEK) or designed adjoint spectra (SEG) to check separately capture or scattering data.

The calculations have been made in 70 energy groups because some considerable differences were found when collapsing to 18 groups. One of the reasons was detected in the very broad 18th energy group (from 10^{-5} until 100.3 eV). In case of facilities with soft neutron spectra, a collapsing to 18 or 7 energy groups is not recommended.

The C/E-values were compared to results obtained with the European scheme and with a cross-wise use of JEF-2.2 and JNC codes. When using different input libraries, codes in the routes, self-shielding treatments, and likewise different energy group structures, it is difficult to locate exactly the source of the differences and deviations in C/E-values. But, considerable differences became apparent in the calculated slowing-down effect. The total scattering effect calculated by the JNC route is mostly larger with a tendency to negative signs. It could not be found out if this fact is due to differences in the adjoint spectra, scattering data, or perturbation calculation.

The C/E-values show that uncertainties in JENDL-3.2 and JEF-2.2 still exist, especially for structural materials and weak absorbers. A good agreement was found for standards and most strong absorbers. Of course, the information is integral; precise corrections should be obtained from adjustment studies. For that purpose, sensitivities in 70 energy groups have been already prepared with SAGEP for all sample materials and facilities.

Precise measurements are very essential; the statistical error is the main component in the error of the C/E-values. Reactor noise and drifts give the lower limit in the measurements. Consequently, integral tests are not recommendable for sample materials with a very small specific reactivity, even if due to large compensating effects.

Integral tests are characterized by the specialty that the reactivity of the sample is often determined mainly by one cross-section type in a special energy range or by a few resonances. These data should be reviewed first. Because of the fact that the calculation is performed in a few steps, calculated averaged transmissions have been proved useful as an additional and complementary method to detect errors in the original data or to compare data libraries [33].

The analyses in this work could easily be repeated for the validation of JENDL-3.3 or JEFF-3.0. In case of STEK, however, the calculation of the self-shielding correction for sample size and extrapolation to the infinitely dilute value CRW should be performed anew using JENDL-3.3 or JEFF-3.0 consistently as used in the route. The two methods of self-shielding treatment (self-shielding factors with interpolation against probability tables/sub-group method) should be compared. The extensive series of measurements of the dependence of the sample reactivity on sample size in SEG facilities could be used for this. At last, more libraries for input and other codes should be used and compared, desirable even cross-wise to get separate information for data or codes.

References

- [1] NEA NSC International Evaluation Cooperation, in "Neutron Nuclear Data Evaluation Newsletters", NNDEN/46, March 1993, p.48
- [2] K.Dietze, G.Rimpault:
An Analysis of Sample Reactivity Measurements in Rossendorf SEG Configurations using the JEF-2 Data Base,
NEA JEF/DOC-451 (1993)
- [3] K.Dietze, E.Fort, S.Rahlfs, G.Rimpault, M.Salvatores:
JEF-2 Data Check by Reanalysis of the Rossendorf Experiments in Reactor Configurations with Specially Designed Adjoint Spectra,
Int. Conf. on Nucl. Data for Sci. and Techn., Gatlinburg, May 9 – 13, 1994,
Proceedings Vol. 2, p.789 (1994)
- [4] A.Meister: Analysis of the Sample Oscillation Measurements in the STEK-facility using JEF-2.2 Data,
NEA JEF/DOC-746 (1998)
- [5] E.Fort, M.Salvatores:
JEF2 Validation, Methodology-Present Results-Future Plans,
Int. Conf. on Nucl. Data for Sci. and Techn., Gatlinburg, May 9 – 13, 1994,
Proceedings Vol. 2, p. 768 (1994)
- [6] M.Kawai, A.Zukeran, T.Nakagawa, S.Chiba, Y.Nakajima, T.Sugi, Y.Kikuchi,
T.Watanabe, H.Matsunobu:
Revision of FissionProduct Nuclear Data for JENDL-3.2,
Int. Conf. on Nucl. Data for Sci. and Techn., Gatlinburg, May 9 – 13, 1994,
Proceedings Vol. 2, p. 727 (1994)
- [7] T.Watanabe, M.Kawai, T.Nakagawa, Y.Nakajima, T.Sugi, S.Chiba, A.Zukeran,
H.Matsunobu, H.Takano, H.Akie:
Benchmark Tests of FP Nuclear Data in JENDL-3.2 and Consideration of Resonance Self-Shielding Effects for Neutron Strong Absorber Nuclei,
Final Report of the JNDC FPND Working Group (1996)
- [8] H.Th.Klippel, J.Smit:
The coupled fast-thermal critical facility STEK,
RCN-209 Petten (1974)
- [9] K.Faehrmann, G.Huettel, H.Krause:
Das schnelle Einsatzgitter (SEG) im Rossendorfer Ringzonenreaktor (RRR),
Kernenergie 3/1974, p.70, in German
- [10] K.Dietze:
The Rossendorf RRR/SEG-Facility (Documentation),
Note Technique CEA CEN Cadarache, NT SPRC/LEPH/93-230 (1993)

- [11] K.Faehrmann, E.Lehmann:
A fast-thermal coupled system with energy-independent adjoint flux,
Kernenergie 24, p. 431 (1981)
- [12] K.Dietze, K.Faehrmann, G.Huettel, E.Lehmann:
Neutron Data Check for Structural Materials by Reactivity Measurements in a
Fast Facility with Energy-independent Adjoint Flux,
Kernenergie 29, 11, p. 401 (1986)
- [13] E.Lehmann, K.Faehrmann, G.Huettel, H.Krause, H.Kumpf:
The method of energy-independent adjoint flux and its perfection by the SEG-5
configuration,
Kernenergie 29, p.30 (1986)
- [14] K.Dietze, K.Faehrmann, W.Hansen, G.Huettel, H.Kumpf, E.Lehmann:
Neutron Absorption Data Analysis by means of Integral Experiments in Fast
Critical Facilities,
Kerntechnik 53/2, p. 143 (1988)
- [15] E.Lehmann, G.Huettel, H.Krause, H.Kumpf:
A fast critical reactor assembly with strong energy dependence of adjoint flux,
Kernenergie 34, p.9 (1991)
- [16] K.Dietze, W.Hansen, G.Huettel, H.Kumpf, E.Lehmann, D.Richter:
Neutron data check by reactivity measurements in critical assemblies with
predetermined adjoint flux,
Int. Conf. on Nucl. Data for Sci. and Techn., Juelich, May 1991, Proc., p. 198
- [17] K.Dietze:
Integral Test of FPND by Reactivity Measurements in Reactor Configurations
with Specially Designed Adjoint spectra,
Spec. Meeting on FPND, Tokai, May 1992, NEA/NSC/DOC(92)9, p.404 (1992)
- [18] J.J.Veenema, A.J.Janssen:
Small-sample reactivity worths of fission product isotopes and some other
materials measured in STEK,
ECN-10 Petten (1976)
- [19] K.Dietze, H.Kumpf:
Eine Analyse der Kerndaten von Spaltprodukten durch Reaktivitaetsmessungen
in schnellen Reaktorkonfigurationen mit energie-unabhaengiger Einflussfunktion,
Kernenergie 34, 1, p. 1 (1991), in German
- [20] A.J.Janssen, H.Gruppelaar, R.J.Heijboer, N.Karouby-Cohen, L.Martin-Deidier,
G.Rimpault, M.Salvatores:
Integral Test of JEF-1 Fission-product Cross Sections,
Part 1, NEA JEF/DOC-50, 1984
Part 2, NEA JEF/DOC-67, 1984

- [21] A.J.Janssen, H.Gruppelaar, N.Karouby-Cohen, M.Salvatores:
Integral test of JEF-1 cross-sections for important fission products,
Vol. 3, NEA JEF/DOC-85, 1985
- [22] A.J.Janssen, H.Gruppelaar, R.J.Heijboer, N.Karouby-Cohen, L.Martin-Deidier,
G.Rimpault, M.Salvatores:
Integral-data Test of JEF-1 Fission-product Cross Sections,
ECN-176 Petten (1985)
- [23] T.Nakagawa, et al.:
Japanese Evaluated Nuclear Data Library Version 3 Revision 2: JENDL-3.2,
J. Nucl. Sci. Techn., 32 (12), 1259 (1995)
- [24] M.Nakagawa, K.Tsuchihashi:
SLAROM: A Code for Cell Homogenization Calculation of Fast Reactor,
JAERI 1294 (1984)
- [25] T.B.Fowler, et al.: Nuclear Reactor Analysis Code: CITATION,
ORNL-TM-2496, Rev.2, (1971)
- [26] M.Nakagawa, J.Abe, W.Sato:
Code System for Fast Reactor Neutronics Analysis,
JAERI-M 83-066 (1983)
- [27] S.Iijima, H.Yoshida, H.Sakuragi:
Calculation Program for Fast Reactor Design, 2, (Multi-dimensional Perturbation
Theory Code based on Diffusion Approximation: PERKY),
JAERI-M 6993 (1977)
- [28] C.J.Dean, C.R.Eaton, P.Peerani, P.Ribon, G.Rimpault:
Production of Fine Group Data for the ECCO Cell Code,
Int. Conf. on the Physics of Reactors, PHYSOR 90, Marseille, Vol.3, P IV-15
(1990)
- [29] M.J.Grimstone, J.D.Tullet, G.Rimpault:
Accurate Treatment of Fast Reactor Fuel Assembly Heterogeneity with the
ECCO Cell Code,
Int. Conf. on the Physics of Reactors, PHYSOR 90, Marseille, Vol.2, IX-24 (1990)
- [30] J.Y.Doriath, C.W.M.Callien, E.Kiefhaber, U.Wehtmann, J.M.Rieunier:
ERANOS1: The Advanced European System of Codes for Reactor Physics
Calculation,
Int. Conf. on Math. Methods and Supercomputing, Karlsruhe, Vol.2, p.177 (1993)
- [31] K.Dietze:
Analysis of the Rossendorf SEG experiments using the JNC route for reactor
calculation,
Report JNC TN9400 99-089, Oarai (1999)

- [32] K.Dietze:
Zur Normierung und Genauigkeit von integralen Experimenten im SEG,
Report RPV-1/89, Research Center Rossendorf (1989), in German
- [33] K.Dietze, P.Ribon. P.Siegler:
Neutron Data Test by Comparison of Calculated and Measured Averaged
Transmissions,
NEA JEF/DOC-777 (1999)
- [34] L.P.Abagyan, N.O.Bazazyants, M.N.Nikolaev, A.M.Tsibulya:
Grupповые константы для расчёта реакторов и защиты,
Energoizdat, Moskva (1981)